JOURNAL OF VIROLOGY, June 2001, p. 5252–5262 Vol. 75, No. 11
0022-538X/01/$04.00+0 DOI: 10.1128/JVI.75.11.5252–5262.2001

Tracking the Spread of a *lacZ*-Tagged Herpes Simplex Virus Type 1 between the Eye and the Nervous System of the Mouse: Comparison of Primary and Recurrent Infection

CAROLYN SHIMELD,[1]* STACEY EFSTATHIOU,[2] AND TERRY HILL[3]

Division of Ophthalmology[1] and Department of Pathology and Microbiology,[3] University of Bristol, Bristol BS8 1TD, and Division of Virology, University of Cambridge, Cambridge CB2 1QP,[2] United Kingdom

Received 5 December 2000/Accepted 2 March 2001

The spread of herpes simplex virus type 1 (HSV-1) during primary ocular infection and after reactivation of latent infection in the trigeminal ganglion (TG) was examined in the mouse using a genetically modified virus containing the *lacZ* reporter gene under the control of the immediate-early 110 promoter. Whole tissue mounts of the eye and lids, their sensory nerves, and TG with the attached dorsal root entry zone (DRE) into the central nervous system (CNS) were stained for β-galactosidase. Sixteen hours after inoculation of the cornea by scarification, staining was found in the scarified epithelium of the cornea and in the unscarified conjunctiva. By 24 h, staining was also seen in a few TG neurons and by 96 h their number had greatly increased and their distribution was more widespread. Stained cells (identified as Schwann cells by their staining for glial fibrillary acidic protein [GFAP] or S-100) in the TG were first seen close to stained neurons at 40 h, and by 48 h lines of such cells extended partway toward the periphery and toward the DRE. By 72 h, these lines had reached the periphery and the DRE where the adjacent CNS was also stained. In the cornea, stained cells with the morphology and arrangement of Schwann cells were seen from 40 to 120 h. After reactivation of latent infection, 10 of 22 samples had positively stained neurons. In eight samples, corneal and lid epithelial cells were stained. No stained Schwann cells were seen in the TG; however, branched networks of such cells were present in the cornea and the lids. This detailed sequential analysis has provided new information on the involvement of Schwann cells in the pathogenesis of primary and recurrent HSV-1 disease in the TG and the cornea.

The ability of neurotropic herpesviruses, such as herpes simplex virus (HSV), to spread in nerves in a retrograde or anterograde direction, has long been recognized (reviewed in reference 8). Although the route used by the virus during such spread was debated for some time, in particular the role of Schwann cells, intra-axonal transport is now generally accepted as the underlying mechanism.

Morphological evidence has suggested that Schwann cells are relatively resistant to infection (4, 6); however, tracts of infected Schwann cells in peripheral nerves associated with the site of primary infection have been described in many experimental studies (reviewed in reference 12). The precise circumstances underlying such infection and the role, if any, of Schwann cells in the pathogenesis of herpetic infection have received little attention. It is noteworthy, however, that in recurrent cutaneous herpetic lesions in humans, there was frequent histopathological evidence of HSV infection in the Schwann cells of nerve twigs with inflammatory infiltrates in and around the nerves (46).

It has been hypothesized (13) that during retrograde transport in the axon the virus would be unable to leave the axon and infect the associated Schwann cells, since it would have lost its envelope during entry into nerve endings in the peripheral tissue (26). It was further suggested that once new enveloped particles have been made in the cell body of sensory neurons, these particles could leave axons, particularly if nonmyelinated, and infect Schwann cells at different points along the nerve tract (13). Obtaining experimental evidence for such events would require studies at different times after infection and probably detailed examination of many serial sections. In a previous study, this demanding requirement was partly overcome by using whole mounts of eye tissue following inoculation of the cornea with HSV (7). Although this method successfully demonstrated by immunocytochemistry the existence of antigen-positive Schwann cells in long tracts of nerves in the eye, the sample did not include the trigeminal ganglion (TG) itself, and therefore early spread of infection along the nerve tract could not be studied. Moreover, because of their large size, the antibody molecules necessary for immunocytochemistry cannot easily penetrate into thicker tissues such as the cornea, so that areas of significant antigen staining may be missed (32). We now describe the use of a genetically engineered virus in which a reporter gene for the bacterial enzyme β-galactosidase (β-Gal) has been inserted into a nonessential gene of HSV-1, Us5, under the control of the promoter of an HSV immediate-early gene, IE110 (22). Both in tissue culture and in vivo, expression of β-Gal occurs during lytic infection and is switched off once latency is established. Moreover, in primary neuronal cultures infected with virus recombinants expressing reporter genes from the IE110 or human cytomegalovirus IE promoters, the percentages of reporter gene-positive neurons

* Corresponding author. Mailing address: Division of Ophthalmology, School of Medical Sciences, University of Bristol, University Walk, Bristol BS8 1TD, United Kingdom. Phone: 44-117-9287627. Fax: 44-117-9287896. E-mail: C.Shimeld@bris.ac.uk.

were similar to the proportions of cells expressing viral antigen (1). This suggests that the detection of the ICP0 reporter gene gives an accurate reflection of viral protein synthesis. However, since the promoter activity would mark cells very early in the lytic cycle (i.e., prior to virus production), we cannot be sure that some cells are not abortively infected.

The production of β-Gal allows detection of virus-infected cells by using reagents which more easily penetrate tissues than antibody. Moreover, we have now developed a more extensive whole mount of tissues which includes not only the eye but also its sensory nerve supply from the TG, the ganglion itself, and the attached entry zone from the ganglion into the brain stem (dorsal root entry [DRE]). The combination of this comprehensive tissue preparation and the tagged virus has therefore allowed us to perform a detailed sequential analysis of the events in different parts of the nervous system and ocular tissues at various times after primary infection and thereby to clarify the involvement of Schwann cells. Moreover, since the tagged virus establishes latency and reactivates in a manner similar to that of the parental strain (22), we have been able to use our model of recurrent ocular disease (34) to make a similar analysis of events following UV-induced reactivation of latent virus in the TG.

MATERIALS AND METHODS

Viruses. Viruses were propagated and assayed on Vero cells. HSV-1 strain SC16 110 *lacZ* was derived from HSV-1 strain SC16 (16) as described previously (22). In brief, virus SC16 110 *lacZ* contains a 968-bp promoter fragment which extends from position −818 to position +150 with respect to the IE110 transcription start site linked to *lacZ* and inserted into the nonessential Us5 locus of HSV-1 strain SC16. When grown in tissue culture, this virus produces blue β-Gal-positive plaques.

Animal models. Specific pathogen-free, 8-week-old female NIH/OLA inbred mice were obtained from Harlan/Olac; they were maintained as a breeding colony in the Department of Pathology and Microbiology. For studies on primary infection, mice were anesthetized with 100 mg of ketamine (Parke-Davies Veterinary, Pontypool, United Kingdom) per kg of body weight and 10 mg of xylazine (Bayer plc, Bury St. Edmonds, United Kingdom) per kg of body weight and inoculated by scarification of the left cornea with a 26-gauge needle (44) through a 5-μl drop of medium containing 10^5 PFU of HSV-1 strain SC16 110 *lacZ* or of HSV-1 strain SC16. Control mice were inoculated in the same way with a preparation of uninfected Vero cells (mock inoculum) made in the same manner as the virus inoculum. For studies on reactivation of latent infection, mice were treated as described above, except that 24 h before infection, animals were inoculated intraperitoneally with human serum (Chemicon International, Temecula, Calif.) containing antibodies to HSV-1 (34). The serum was diluted in phosphate-buffered saline (PBS) to give a 50% effective dose of 8,000. Passive immunization is used to protect the eye from the severely damaging effects of HSV-1 disease (35). At least 35 days after inoculation of virus, mice were anesthetized and placed with the left eye proptosed below a Hanovia lamp (emitting a peak of 4.02 mJ/cm^2 s at 320 nm), and the left cornea and lids were irradiated for 90 s.

Examination of eyes and isolation of virus from eyewashings. Mice were anesthetized, and the cornea, iris, and lids were examined for signs of disease using a slit lamp microscope. Eyewashings were taken and put onto Vero cells for the isolation of virus (44). For studies on primary infection, clinical examination and isolation of virus was done immediately before mice were killed. For studies on reactivation of latent infection, these procedures were performed immediately before UV irradiation and on each of days 1 to 4 after such treatment.

Dissection of tissues for β-Gal staining. Anesthetized mice were perfused with 2% paraformaldehyde containing 0.2% glutaraldehyde. A block dissection was made of the left TG with its following attachments: DRE, ophthalmic nerve (lacrimal, frontal, and nasociliary branches), maxillary nerve, optic nerve, eyeball, conjunctiva, and upper and lower eyelids. The TG consisted of its three parts: ophthalmic (TG1), maxillary (TG2), and mandibular (TG3). To facilitate penetration of the staining reagents into the eyeball, the lens was removed via a limbal incision. A schematic of the block dissection is shown in Fig. 1A.

Histochemical detection of β-Gal. β-Galactosidase was detected as described previously (21). In brief, tissues were fixed for 1 h on ice in 2% paraformaldehyde containing 0.2% glutaraldehyde. They were then washed twice in detergent solution (0.01% sodium desoxycholate, 0.02% Nonidet P-40, 2 mM $MgCl_2$ in PBS) and left on ice in this solution for 30 min. Tissues were then incubated at 37°C for 3 to 4 h in X-GAL solution (detergent solution containing 4.5 mM potassium ferricyanide, 4.5 mM potassium ferrocyanide and 1 mg of 5-bromo-4-chloro-3-indolyl-β-D-galactopyranoside [X-Gal] per ml), transferred to 20% glycerol in PBS for 1 h at 4°C, and then incubated overnight at this temperature in 50% glycerol in PBS. While being viewed through an operating microscope, the anterior segment (cornea, sclera, and iris), including a small amount of bulbar conjunctiva, was dissected away from the eye and incisions were made in the eyelids to allow the tissues to be laid flat on glass microscope slides. They were mounted in Apathy's medium, and the coverslips were sealed with nail varnish.

Positive and negative staining controls were included in each run. These were monolayers of Vero cells on coverslips which were infected with 30 PFU of HSV-1 SC16 110 *lacZ* and incubated for 48 h. Coverslips were fixed in 0.5% glutaraldehyde for 15 min, and after washing they were incubated with detergent solution for 5 min. Positive controls were then stained with X-GAL solution as described above and negative controls were stained with diluent alone.

In a preliminary experiment, tissue taken from animals infected 120 h previously was stained for β-Gal expression. Tissues were then rapidly dehydrated and embedded in paraffin wax. Serial sections were cut and counterstained with neutral red. Examination of the sections showed positive staining throughout the entire TG, confirming the penetration of the staining reagents into the thickest part of the tissue block.

EM. To facilitate location of infected cells, tissue samples were taken from mice 120 h after inoculation of the cornea with HSV-1 SC16 110 *lacZ* (when numbers of infected Schwann cells were at a maximum). The blue-stained tracts of cells in the ophthalmic nerve were dissected out and then fixed overnight in sodium cacodylate buffer containing 2.5% glutaraldehyde. However, tissues prepared in this way had poor morphology when observed by electron microscopy (EM). Further studies where the 2% paraformaldehyde containing 0.2% glutaraldehyde fixative used in the β-Gal staining was replaced by a fixative used for EM preparations, sodium cacodylate buffer containing 2.5% glutaraldehyde, failed to improve the morphology. However, similar numbers of β-Gal-positive cells were seen after use of either fixative, suggesting that the increase in concentration of glutaraldehyde had not reduced the sensitivity. The best morphology was found in samples from mice perfused with sodium cacodylate buffer containing 2.5% glutaraldehyde followed by overnight incubation at 4°C in this fixative but unstained for β-Gal. In all cases, tissues were finally postfixed in osmium and embedded in LR White. Ultrathin sections, at several levels across the nerve, were stained with uranyl acetate and lead citrate and examined by transmission EM.

Identification of Schwann cells using antibodies to GFAP or S-100 protein. Antibodies to glial fibrillary acidic protein (GFAP) and S-100 were chosen, since these mark glial cells, including Schwann cells. Block dissections from six mice infected on the cornea 120 h previously with HSV-1 SC16 110 *lacZ* were prepared and stained for β-Gal as described above. Two samples were postfixed overnight in 2% paraformaldehyde containing 0.2% glutaraldehyde and then dehydrated and embedded in paraffin wax. Serial 6-μm sections were cut. The remaining four samples were stained as whole mounts, and to facilitate penetration of the antibodies into the corneal stroma, 10 radial full-thickness incisions were made into the corneas. These whole mounts and the sections were stained by the avidin-biotinylated horseradish peroxidase complex (ABC) method using the following reagents in sequence: 3% hydrogen peroxide, 20% normal goat serum, rabbit anti-GFAP serum (DAKO) diluted 1:500 or rabbit anti-S-100 serum (Sigma) diluted 1:800, biotinylated goat anti-rabbit (Vector) diluted 1:50 and preabsorbed with normal mouse serum, ABC (Vector), and diaminobenzidine (Vector). Samples were washed three times in PBS between steps. Negative control samples were incubated with normal rabbit serum at the same concentrations as the respective primary antibodies.

Examination of slides and measurement of areas of staining. Whole mounts were examined using 4×, 10×, 20×, and 40× objectives. Tissue sections were examined using 40× and 100× objectives. Areas of β-Gal staining in the corneal epithelium were measured using a Quantimet 500 Image Analysis system (Leica, Cambridge Ltd., Cambridge, United Kingdom). Normal probability plots showed that the data conformed to a normal distribution and thus allowed comparisons by analysis of variance. Multiple unplanned comparisons were made by the method of Tukey (39); the level of significance was set at 5%.

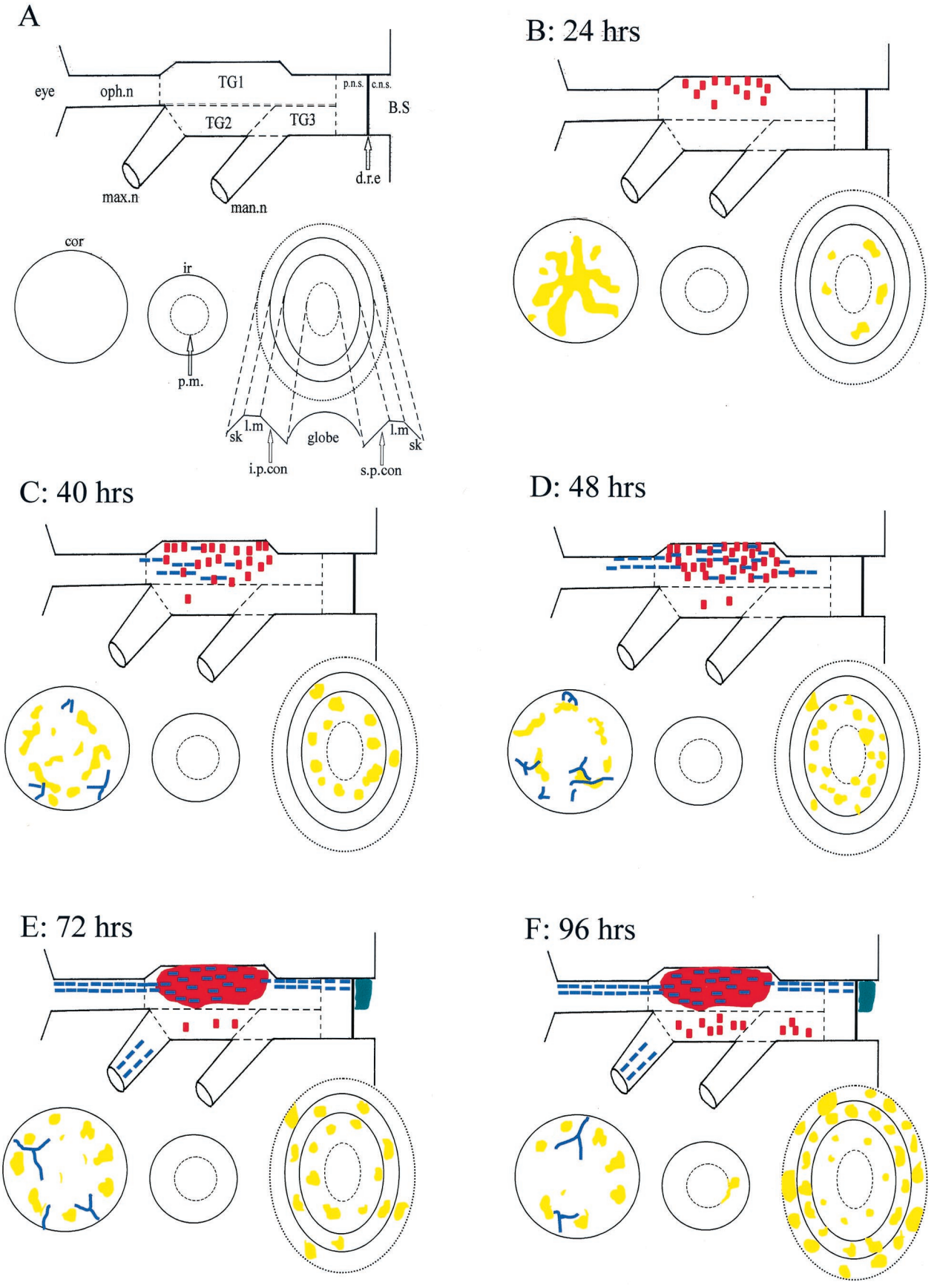
A
eye
oph.n
TG1
TG2
TG3
p.n.s.
c.n.s.
B.S
d.r.e
max.n
man.n
cor
ir
p.m.
sk
l.m
globe
l.m
sk
i.p.con
s.p.con
B: 24 hrs
C: 40 hrs
D: 48 hrs
E: 72 hrs
F: 96 hrs

RESULTS

Primary infection. (i) Experimental protocol. Four mice inoculated with HSV-1 strain SC16 110 *lacZ* and one given mock inoculum were taken on each of the following hours after inoculation: 16, 24, 40, 48, 72, 96, 120, and 168. In addition, one mouse inoculated with the parental virus, HSV-1 strain SC16, was taken at 120 h. Mice were examined for clinical disease and eyewashings were taken for the isolation of virus, and then the animals were killed and their tissues were removed and processed for β-Gal staining.

(ii) Eye disease and isolation of virus from eyewashings. Sixteen hours after inoculation of HSV-1 strain SC16 110 *lacZ*, all mice had multiple corneal epithelial ulcers, some punctate and some linear, and by 24 h these ulcers were larger and underlaid by haze. At 40 and 48 h, animals had large central corneal ulcers, iris hyperemia, and enlargement of the limbal vessels. By 96 h, corneas had more severe haze or opacity and animals had swollen lids which, by 120 h, had progressed to lid disease (ulcers and scabs). Eyewashings at all timepoints from 16 to 168 h yielded large amounts of virus (>100 PFU/eye).

(iii) Identification of types of infected cells. In whole mounts, infected (blue-staining) Schwann cells were identified by their characteristic long thin shape and end-to-end arrangement, usually in tracts, following the predicted course of nerves and more intense staining around their nuclei. In tissue sections, cells in the ophthalmic and maxillary nerve tracts after inoculation of the cornea 120 h previously with HSV-1 were confirmed to be Schwann cells by their double staining for β-Gal and either GFAP (Fig. 2A1) or S-100 and by the EM of ultrathin sections (see below). Attempts to apply the double-staining method to identify corneal Schwann cells in whole mounts were disappointing. No cells stained positively for GFAP or S-100 were seen, most likely due to poor penetration of the antibodies into this relatively thick tissue. We were therefore unable to identify unequivocally the infected Schwann cells of corneal nerves.

(iv) Identification of HSV-1-infected Schwann cells by EM. In the ophthalmic nerve taken from mice 120 h after inoculation of the corneas with HSV-1 SC16 110 *lacZ*, nuclei with marginated chromatin and intranuclear herpes capsids were seen in several sections. Such cells were identified in the tissues from two mice processed for EM after β-Gal staining and in a further two after conventional fixation for EM. As expected, the tissue preservation was much better in the latter. At one end of the nerve fragment, presumably at the edge of the ganglion, a few neurons were seen, readily identified by their characteristic morphology and the closely apposed satellite cells. Some of these neurons showed the signs of herpetic infection mentioned previously. All other herpes-infected cells (a total of approximately three to four per section) had characteristics of Schwann cells, viz., an elongated shape and a basement membrane covering the plasma membrane (Fig. 3). Moreover, all such cells were nonmyelinating Schwann cells with naked axons in their cytoplasm and none showed evidence of virus capsid envelopment.

(v) Assessment of β-Gal staining in tissues. No β-Gal-positive staining was seen in samples from mock-inoculated mice or in the sample taken from a mouse 120 h after infection with HSV-1 strain SC16, the untagged parental virus, which lacks the reporter gene. The incidence and distribution of β-Gal-positive staining in the tissues tested on successive timepoints after inoculation of HSV-1 strain SC16 110 *lacZ* are shown in Table 1. A diagrammatic representation of staining in whole tissue mounts at different times after inoculation of the cornea with HSV-1 SC16 110 *lacZ* is shown in Fig. 1B through F. In samples from control and infected mice the level of background staining was extremely low; however, some pale nonspecific staining was seen in the meibomian glands of the eyelids (Fig. 2B2).

(vi) Staining in the corneal epithelium. Sixteen hours after infection, all mice had large numbers of intensely stained corneal epithelial cells (Table 1). The pattern of distribution of stained cells resembled the scarification lines made during the inoculation procedure, with the majority of staining in the central cornea (Fig. 2B1). At 24 h (Fig. 1B), the areas of staining in the corneal epithelium had increased to an average of 2.3 mm^2, whereas the pattern and intensity of staining was similar to that seen at 16 h. By 40 h, the intensity of staining had declined and the area of staining in the corneal epithelium had decreased significantly ($P < 0.05$) to an average of 0.7 mm^2. Moreover, the pattern of distribution of such staining had changed, with positive cells surrounding a large central unstained area which corresponded with the central corneal epithelial ulcer seen clinically. At 96 and 120 h, foci of intensely stained cells appeared, peripheral to the fading central ulcers (Fig. 1F). These account for the slight increases in the areas of stained corneal epithelial cells seen at these timepoints (an average of 0.9 mm^2). Similar foci were still present at 168 h.

(vii) Staining in corneal nerves. Three of four samples taken at 40 h had staining in single or thin bundles of lines of cells morphologically resembling Schwann cells of corneal nerves (Table 1; Fig. 1C). Contiguous stained lines stretched through the bulbar conjunctiva and sclera into the cornea and these often branched at the limbus. At 48 and 72 h, all samples had such staining and the lines of cells had become more numerous and thicker, and their branches formed a network of stained Schwann cells in the cornea. These networks were particularly

FIG. 1. Diagrammatic representation of β-Gal staining in whole tissue mounts (ocular structures, their trigeminal nerve supply, the trigeminal ganglion, and its root in the brain stem) at different times after inoculation of the cornea with HSV-1 SC16 IE110 *lacZ*. (A) Key to diagram. In the mounted specimen, the part containing the conjunctiva, lids, and skin (lower right in panel A) remains attached to the ophthalmic nerve, but for clarity this is drawn separately. Similarly, in the specimen, the iris (lower center in panel A) is a part of the anterior segment but again, for clarity, this is drawn separately. TG1, ophthalmic part of the trigeminal ganglion; TG2, maxillary part; TG3, mandibular part; oph. n, ophthalmic nerve; max. n, maxillary nerve; man. n, mandibular nerve; B.S, brainstem; d.r.e, dorsal root entry zone; cor, cornea; ir, iris; p.m., pupillary margin; sk, skin; l.m, lid margin; i.p. con, inferior palpebral conjunctiva; s.p. con, superior palpebral conjunctiva. In panels B through F, the colored areas indicate cells or regions with β-Gal staining: red, individual neuronal cell bodies (where such cells were too numerous to count, the region involved is represented as a larger red area); blue dashed lines, Schwann cells; yellow, areas of staining in epithelial tissues (cornea, conjunctiva, skin) and iris; blue-green, staining in the CNS.

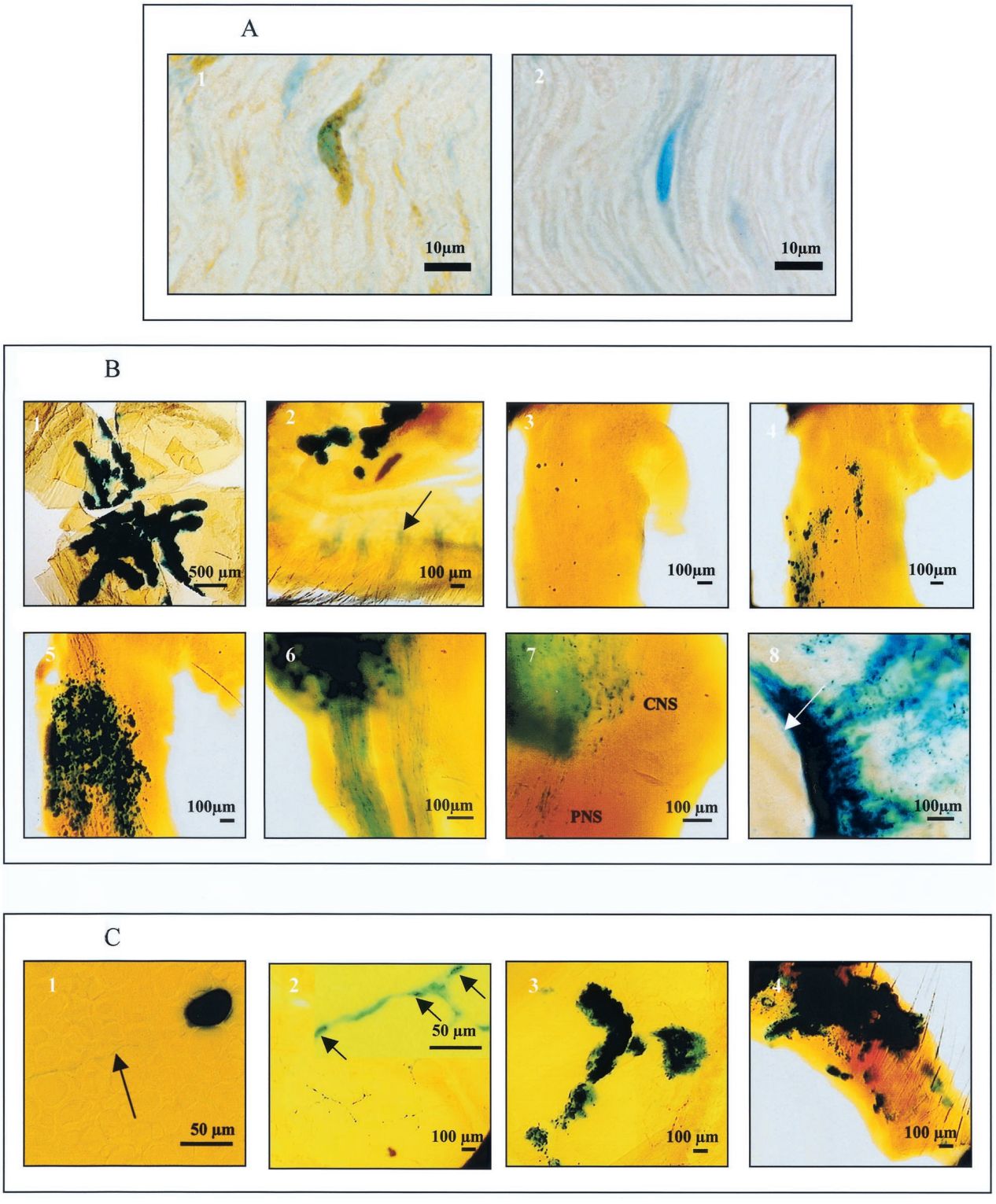

FIG. 2. (A) Histochemical detection of β-galactosidase and immunohistochemical detection of GFAP in mouse ophthalmic nerve 120 h after inoculation of the cornea with HSV-1 SC16 110 *lacZ*. Panel 1 shows a β-galactosidase (blue) and GFAP (brown) double-positive cell; panel 2 shows a β-galactosidase-positive cell stained as for panel 1, except that the anti-GFAP antibody was replaced by normal rabbit serum. (B) Histochemical detection of β-galactosidase in mouse tissues at different timepoints after similar inoculations (1 through 8). Expression was detected in the corneal epithelium (1) and the superior palpebral fornix of the conjunctiva (2) at 16 h after inoculation (the arrow marks nonspecific staining of meibomian glands), isolated neurons in the TG 24 h after infection (3), small groups of neurons, satellite cells, and Schwann cells in the TG 48 h after inoculation (4), large numbers of neurons, satellite cells and Schwann cells in the TG 72 h after infection (5), Schwann cells of the ophthalmic nerves 96 h after infection (6), the CNS at the DRE and Schwann cells in the PNS 120 h after infection (7) and the iris 120 h after inoculation (8) (arrow marks pupillary margin). (C) Histochemical detection of β-galactosidase in mouse tissues at different timepoints after reactivation of

prominent in the periphery of corneas and lay below stained corneal epithelial cells as judged by the plain of focus. By 120 h, staining of these networks was scanty, and at 168 h no such staining was seen.

(viii) Staining in the iris. β-Gal-positive staining was seen in the iris only in samples taken 96 and 120 h after inoculation (Table 1). Stain was seen along the edge of the pupillary margin and sometimes in patches in the main body of the iris (Fig. 2B8).

(ix) Staining in the conjunctiva. All samples taken at 16 h had small foci of β-Gal-positive cells in the superior palpebral fornix (Fig. 2B2). By 24 h, the amount of staining in this tissue had increased and foci of positive cells were also detected in the inferior palpebral fornix (Fig. 1B), and many of the foci had developed central holes and resembled ulcers. The areas of positively stained conjunctival cells increased dramatically by 48 h, and many of the infected cells were in the conjunctiva that overlaid both tarsal plates. Between 72 and 168 h, the amount of β-Gal staining in the conjunctiva declined.

(x) Staining in the lids. Infected cells in the lid margins first appeared at 40 h after inoculation when two of four samples had small numbers of foci (one to three) of β-Gal-positive staining (Table 1). By 72 h, the lids of all samples had foci of positive cells, many of which appeared to be closely associated with hair follicles. The amount of staining in lid margins increased, and all samples tested at 96 and 120 h had almost continuous staining around the entire lid margins (Fig. 1F). At 168 h, the amount of staining had decreased.

(xi) Staining in the TG and DRE. No β-Gal-positive staining was detected in the TG 16 h after inoculation (Table 1). By 24 h, all samples had positive staining in small numbers (3 to 20 per TG) of isolated neuronal cell bodies in TG1 (Fig. 1B and 2B3). By 40 h after inoculation, infection had progressed in all samples to larger numbers of neuronal cell bodies (30 to 100 per TG) and some of their associated satellite cells. Many of the stained neuronal cell bodies and satellite cells were in small clusters and their distribution was more extensive than that seen at 24 h with some stained cells in the part of TG2 bordering TG1 (Fig. 1C and 2B4). Single lines of β-Gal-positive stained Schwann cells extended from positively stained neuronal bodies. In all samples, these lines extended towards the periphery and into the ophthalmic nerve. In contrast, the lines extending centrally were much shorter. This, and other staining of this type in other sites, was identified as being within Schwann cells by the criteria described previously. However, in all cases it is impossible to tell whether or not such staining in nerve tracts also included some contribution from β-Gal within the axons. By 48 h, lines of stained Schwann cells extended to the peripheral nervous system (PNS) side of the DRE and those in the ophthalmic nerve consisted of bundles of stained Schwann cells (Fig. 1D). Far smaller numbers of TG2 Schwann cells stained for β-Gal; however, such stained cells were seen in the peripheral part of the maxillary nerve. These were first detected at 72 h after inoculation and were still present at 168 h. Small areas of positive staining were first detected in the CNS at the DRE at 72 h in three of four samples tested. At 120 and 168 h all samples had larger areas of such staining (Table 1) and the majority of staining was diffuse, with only small numbers of stained cells visible (Fig. 2B7). At this time, the numbers of stained neurons in TG1 were too large to count (Fig. 1E and 2B5), and large bundles of stained Schwann cells were seen extending from these neurons along the length of the ophthalmic nerve and in the PNS side of the DRE up to the junction. β-Gal staining was first detected in neuronal cell bodies in TG3 in one of four samples taken 96 h after inoculation of virus (Fig. 1F). There was no evidence of Schwann cell staining in TG3 or in the small portion of mandibular nerve available for examination. At 96 h, staining was also seen in large bundles of Schwann cells forming three tracts within the ophthalmic nerve (Fig. 2B6). These tracts could be traced from stained neuronal cell bodies in TG1 and TG2 to the eyelid margins and tarsal conjunctiva, where they were sometimes seen to branch. These three tracts are likely to be the frontal, nasociliary, and lacrimal branches of the ophthalmic nerve. Occasionally, small branches from one of the tracts were seen entering the eye near the optic nerve. By 168 h, the number of positive neurons had declined to 12 to 50 per TG. The majority of these cells were in TG1 and TG2 and were stained intensely, suggesting recent infection.

Reactivation of latent infection. (i) Experimental protocol. Twenty-two latently infected mice and four mice given mock inoculum were treated with UV irradiation as described above. Eyewashings were taken for the isolation of virus before UV irradiation and on each of days 1 to 4 afterwards. On each of these days, four to seven latently infected mice and one control mouse were killed and their tissues were removed and processed for β-Gal staining. Six latently infected animals were killed before UV irradiation and treated similarly. Eyes were examined for signs of disease prior to UV irradiation and on the day they were killed.

(ii) Eye disease and isolation of virus from eyewashings. Prior to UV irradiation, all eyes were normal. After treatment, transient corneal epithelial ulceration developed and resolved by day 3. In latently infected mice, recurrent dendritic keratitis was seen in one animal on day 3. Recurrent lid disease was seen in one mouse on day 3 and two on day 4. No virus was isolated from the tears of mice prior to UV irradiation or on day 1 after irradiation. Two animals shed virus on a single day, one on day 2 and one on day 3. One mouse shed virus on day 2 and day 3 (Table 2).

(iii) Assessment of β-Gal staining in tissues. No β-Gal-positive staining was seen in samples taken from mock-inoculated UV-irradiated mice or from the six latently infected animals sampled before UV irradiation. The pattern of β-Gal-positive staining in tissues from latently infected mice tested on successive timepoints after UV irradiation is shown in Table 2. The level of background staining was similar to that described previously.

latent virus in the TG by UV irradiation of the cornea: a reactivating neuron in TG1 2 days after irradiation of the cornea (the arrow marks axonal staining) (1), a network of corneal nerve Schwann cells 2 days after UV irradiation (the inset shows apparent nuclear staining in Schwann cells [arrows], at higher magnification) (2), a dendritic lesion of the corneal epithelium 3 days after irradiation (3), and a lesion of the eyelid margin 3 days after irradiation (4).

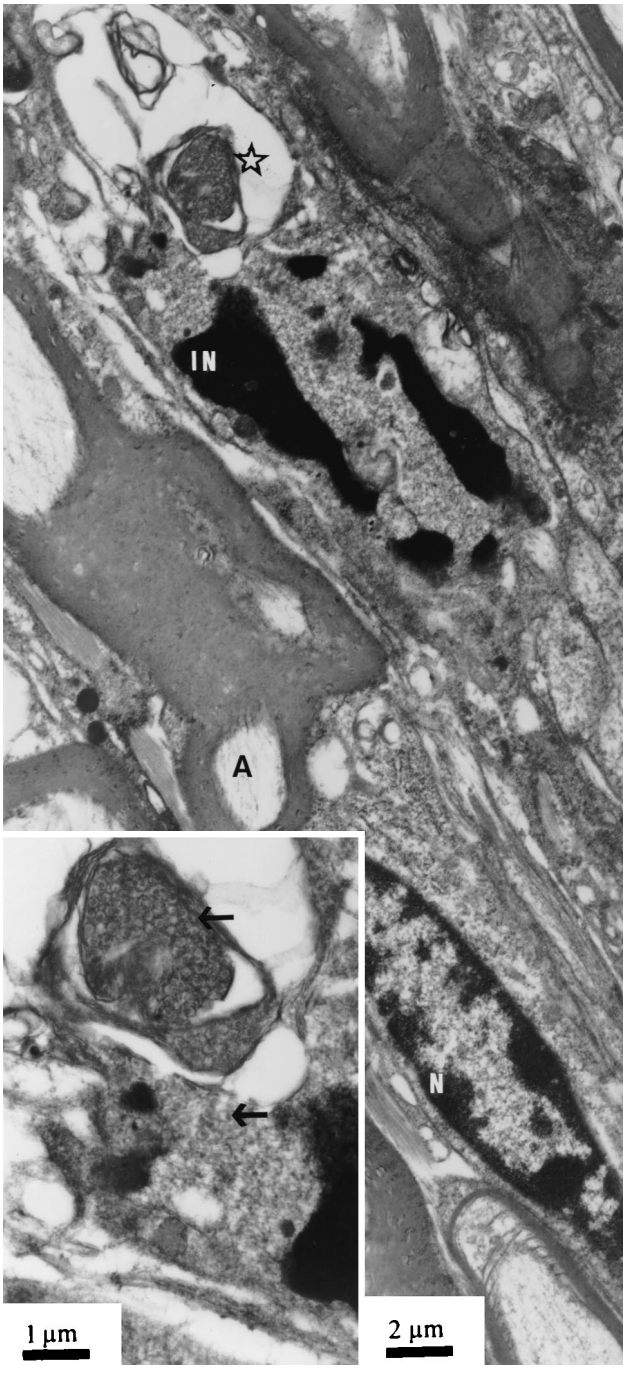

FIG. 3. Ophthalmic nerve 120 h after inoculation of HSV-1 SC16 IE110 *lacZ*. N, uninfected nucleus of myelinating Schwann cell; A, myelinated axon; IN, nucleus of unmyelinated Schwann cell with marginated chromatin. The inset shows area of infected nucleus at higher magnification. Arrows indicate virus capsids.

(iv) Staining in the TG and DRE. β-Gal-positive staining was seen only in neurons. Ten of the 22 TG taken after UV irradiation had such staining. Nine of these had a single stained neuron and one sample had two stained cells. Stained neurons were seen at all time points after UV irradiation, with the maximum incidence on day 1 when four of four samples had positive cells (Table 2). All stained neurons were within TG1, with four located in the rows of neuronal cell bodies that lie at the medial edge of this ganglion, six were deeper in TG1, and one was close to the border between TG1 and TG2. Of the 11 β-Gal-positive neurons, 9 had intense uniform staining over the entire cell body and 2 had discrete punctate staining. One cell with uniform staining also had staining in its axon. The path of this axon, traced by differential focusing, left the cell body in a lateral direction and then turned towards the periphery (Fig. 2C1).

(v) Staining in the cornea and the lids. β-Gal staining was seen in epithelial cells and in branched networks of cells with the morphology and arrangement of Schwann cells in the cornea (Fig. 2C2) and the lids. The amount of positively stained corneal epithelial cells varied from one cell in a sample taken on day 1 to foci of cells in samples taken on later days. One eye from day 3 had dendritic ulcers (see above). The pattern and position of the ulcers and β-Gal staining in the corneal epithelium of this eye were the same (Fig. 2C3). Stained corneal nerves were identified as early as day 1 and were seen in some samples at all timepoints tested. The extent of staining of these nerves varied from a few Schwann cells to a network of cells covering half the cornea (Fig. 2C2). Positive staining of nerves and epithelial cells were seen in two corneal samples, one on day 1 and the other on day 3 (Table 2).

β-Gal staining in lid epithelium was first seen on day 3, when three of seven samples were positive. Positive staining in this tissue was focal and appeared to be associated with hair follicles (Fig. 2C4). The number of foci varied from one to many involving the entire lid margin. On some samples with lid disease, stained Schwann cells were seen in close association with foci of β-Gal-positive lid epithelial cells.

DISCUSSION

In previous studies, SC16 110 *lacZ* and the parental virus SC16 showed similar patterns of infection in mice following cutaneous infection (22), and in the present studies, following primary infection in the cornea, the two viruses produced similar ocular diseases. Although the product of gene Us5 may be antiapoptotic (18), our results provide further evidence that lack of this product (the putative glycoprotein gJ) has no significant effect on host-virus interactions (22), at least in the mouse.

As expected, following inoculation of the cornea with SC16 110 *lacZ*, extensive β-Gal staining was seen as early as 16 h (the first time tested) in the scarified epithelium. Less expected at this early time was the marked staining in the fornix of the upper palpebral conjunctiva, an unscarified area. By 48 h, this staining involved the entire palpebral conjunctiva of both lids. This strongly suggests that the conjunctiva, unlike the cornea, can be infected by some strains of HSV without necessarily suffering damage to its epithelium. This involvement of the conjunctiva may also explain the observed ability of strain SC16, but not strain McKrae, to produce ocular infection in mice without corneal scarification when used at high doses (19).

As made manifest by β-Gal staining of neurons, virus first arrived in the TG between 16 and 24 h after inoculation of the cornea. At this time, β-Gal expression in the TG was limited to

TABLE 1. Incidence of β-Gal expression in the sensory nervous system and ocular tissues after primary infection of mouse corneas with HSV-1[a]

Time after inoculation (h)	No. of mice with staining in indicated tissue/total tested										
	Corneal epithelium	Corneal nerves[b]	Iris	Conjunctiva	Lids	TG1[c]	TG2[d]	TG3[e]	CNS at DRE[f]	Ophthalmic nerve[b]	Maxillary nerve[b]
16	4/4	0/4	0/4	4/4	0/4	0/4	0/4	0/4	0/4	0/4	0/4
24	4/4	0/4	0/4	4/4	0/4	4/4	0/4	0/4	0/4	0/4	0/4
40	4/4	3/4	0/4	4/4	2/4	4/4	1/4	0/4	0/4	0/4	0/4
48	4/4	4/4	0/4	4/4	1/4	4/4	2/4	0/4	0/4	4/4	0/4
72	4/4	4/4	0/4	4/4	4/4	4/4	1/4	0/4	3/4	4/4	4/4
96	4/4	2/4	2/4	4/4	4/4	4/4	4/4	3/4	3/4	4/4	3/4
120	4/4	3/4	3/4	4/4	4/4	4/4	4/4	3/4	4/4	4/4	3/4
160	4/4	0/4	0/4	4/4	4/4	4/4	4/4	4/4	4/4	4/4	4/4

[a] 10^5 PFU of HSV-1 strain SC16 110 *lacZ*.
[b] Staining in Schwann cells.
[c] TG1, ophthalmic part of trigeminal ganglion.
[d] TG2, maxillary part.
[e] TG3, mandibular part.
[f] DRE, dorsal root entry zone.

a small number of neurons, all within TG1, the part supplying sensory nerves to the inoculation site. At these early times, during the period the first virus was being transported along the nerve from the cornea to the ganglion, no β-Gal expression was seen in Schwann cells along the nerve tract. This confirms the generally accepted view that such cells play no part in transport of virus during this period and that axonal flow is the likely route of virus spread.

The absence of Schwann cell staining at this time also supports the suggestion that these cells are unlikely to become infected during retrograde transport (13) since the intra-axonal virions will have lost their envelopes as a result of membrane fusion at the nerve endings (26). Schwann cell staining was also absent during the movement of virus in the opposite direction, along nerves to the eye from reactivated infection in TG neurons. In this case, however, the virus being transported is likely to be enveloped. Nevertheless, the chances of Schwann cells becoming infected may be low since only small amounts of virus appear to be produced as a result of reactivation (37) and the axon involved may be myelinated.

The nerve tract from the cornea to the middle of the ophthalmic division of the TG is about 8 mm long, which means the rate of retrograde axonal flow of virus in trigeminal nerves was approximately 0.4 mm/h. In previous studies of HSV and pseudorabies virus with different nerves (of the hind limb or pinna of the ear), the rate of retrograde flow was estimated to

TABLE 2. Pattern of β-Gal expression in TG and ocular tissue and isolation of virus in eyewashings after reactivation of latent HSV-1 in the mouse TG

Mouse no.	Days after UV irradiation[a]	β-Gal expression in:					Day(s) when eyewashings yielded virus
		TG1[b]	Corneal epithelium	Corneal nerves[c]	Lid epithelium	Lid nerves[c]	
1	1	+	−	−	−	−	
2	1	+	−	−	−	−	
3	1	+	+	+	−	−	
4	1	+	−	−	−	−	
1	2	+	−	+	−	−	
2	2	+	−	−	−	−	
3	2	−	−	−	−	−	
4	2	−	−	−	−	−	
5	2	−	−	−	−	−	
1	3	−	−	+	−	−	
2	3	−	−	−	+	−	
3	3	+	+	+	+	+	
4	3	−	+	−	+	−	
5	3	−	−	−	−	−	
6	3	−	−	−	−	−	
7	3	−	−	−	−	−	
1	4	+	−	−	−	−	
2	4	+	−	−	+	+	3
3	4	−	−	+	−	−	2,3
4	4	+	+	−	−	−	
5	4	−	−	−	−	−	2
6	4	−	−	−	−	−	

[a] On day −1, 0 of 6 mice had β-Gal expression.
[b] TG1, ophthalmic part of trigeminal ganglion.
[c] Staining in Schwann cells.

be slightly faster, about 2 mm/h (4, 9, 10, 20, 28). The rate of flow of virus in the opposite direction, after reactivation in the TG, must be very similar, since in some samples with β-Gal-positive neurons at 24 h after UV irradiation staining in what were probably Schwann cells of corneal nerves was also present.

The number of β-Gal-positive neurons in TG1 became uncountable by 72 h after inoculation. Eventually, such neurons also appeared, but in much smaller numbers, in the other divisions, first in the TG2 at 40 h and then in TG3 by 96 h. This spread of infection within the TG, perhaps involving the "back-door route", has been described and discussed previously (36, 42, 43). With respect to the ganglion itself and the main nerve tracts from the ganglion, β-Gal expression in cells morphologically resembling Schwann cells was first seen at 40 h in close proximity to β-Gal-positive neurons in the ophthalmic division. Such staining extended for a short distance, within the ganglion, along nerve tracts from TG1 toward the periphery and toward the CNS. By 72 h, this staining had extended in both directions, as far as the eye and the junction of PNS and CNS. At 120 h, when the putatively infected Schwann cells were highest in number and therefore easier to locate in sections of tissue, these cells were unequivocally identified as Schwann cells by their double staining with β-Gal and GFAP or S-100, markers known to be present in such cells and other glia (29). The timing (after neurons were infected) and pattern (progressively away from infected neurons in the ganglion) of this Schwann cell involvement support the hypothesis that these cells can become infected following a productive replication cycle in the neuronal cell body, the flow of virus out along axons, and then the emergence of such virus into associated Schwann cells along the nerve tract. It has been argued that this emergence of virus into Schwann cells is more likely if the virus being transported is enveloped (13). It should be noted, however, that the state of virus during such anterograde flow is controversial (reviewed extensively in reference 8). Studies of an in vitro ganglion culture system with one strain of HSV-1 indicate that virus moving in an anterograde direction lacks an envelope (31), and indeed, in this system, viral glycoproteins seem to be transported separately (17). However, and perhaps more significantly, several in vivo studies with different strains of HSV and pseudorabies virus clearly show enveloped particles in transport vesicles within axons of nerves (3, 9, 14, 23). A suggested correlation between the virulence of different virus strains and the state of the transported virus, virulent in vesicles or avirulent as naked capsids (8), has yet to be proven.

We have also suggested that the emergence of virus during axonal transport is much more likely to occur from nonmyelinated axons where the barrier of a myelin sheath is absent (13). The wrapping of more than one nonmyelinated axon by a single Schwann cell would also increase the chance of such cells becoming infected. This predilection for infection in nonmyelinating Schwann cells is supported by EM of the sciatic nerve in mice infected with either HSV (4, 6) or pseudorabies virus (9), another highly neurotropic herpesvirus, in the hind footpad. In the present study, these observations were confirmed by EM of the ophthalmic nerve 5 days after inoculation. Other observations also suggest the importance of peptidergic neurons (which characteristically have nonmyelinated axons) in the pathogenesis of HSV infection (11, 24, 27, 40). In common with previous EM studies of infection in Schwann cells (4, 6), our observations of the lack of any capsid envelopment confirms the suggestion that these cells, like satellite cells (15, 45), are relatively resistant to infection with HSV-1.

The other notable site of Schwann cell infection was in the cornea itself. The ability to detect the pattern and presence of such staining clearly illustrates the very significant advantage of the whole mount of the ocular and neural tissues. In primary infection, stained Schwann cells were seen in fine-branching lines, presumably covering the branching nerve fibers in the plexus under the corneal epithelium, as early as 40 h after inoculation. After reactivation of virus in TG neurons, such Schwann cell staining was also seen but as early as 24 h after irradiation of the cornea. Two possible scenarios could explain how corneal nerve Schwann cells could become infected: (i) by spread of infection from the epithelium into the boundary between the epithelium and the stroma, where the nerves are situated, or (ii) by virus travelling down axons from infected neurons in the ganglion. With respect to the corneal Schwann cell staining seen so early after reactivation of virus in the TG, significant epithelial β-Gal staining did not occur until after 24 h and therefore could not be the source of virus infecting Schwann cells. Therefore, leaving aside the possibility of any corneal latency (5), infection of Schwann cells could only have occurred from virus which had travelled down the axons of neurons in which reactivation had occurred. In the case of primary infection, the later involvement of corneal Schwann cells and the extension, from the periphery, of tracts of infected Schwann cells in mandibular nerves may be indicative of the first scenario (infection by spread from the epithelium into subepithelial nerves). Alternatively, in primary infection, as in reactivation, Schwann cells in the cornea might become infected as a result of anterograde flow of virus from productively infected ganglionic neurons (2). The particular susceptibility of the corneal Schwann cells to infection may, as discussed above, relate to the lack of a myelin barrier, in this case in all the nerves under the corneal epithelium (30, 47).

In the case of reactivated infection, it is noteworthy that the striking dendritic pattern of Schwann cells expressing β-Gal in the cornea occurs as early as 24 h after UV irradiation in some mice and that this precedes the time at which the overlying and similar pattern of dendritic infection occurs in the corneal epithelium. Hence, this may provide further circumstantial evidence to support the view that the dendritic corneal ulcer, so pathognomic of recurrent herpetic infection in the eyes of humans and mice (34), may occur as a result of an "imprinting" from a slightly earlier and anatomically defined pattern of infection in nerves which lie under and very close to the epithelium (25).

In contrast to a previous report using a different mouse strain and a different route of inoculation (41), we found no neurons expressing β-Gal in latently infected unirradiated animals at least 35 days after infection with HSV-1 SC16 110 *lacZ*. However, in our study, passive immunization was used prior to inoculation of virus, a treatment which curtails the spread and subsequent establishment of latency in the TG (35); this may also influence the pattern of β-Gal expression during latency.

In our previous experiments of UV-induced reactivation in the TG (34, 37, 38), we have used the McKrae strain of HSV-1.

From these experiments and other reports using a different mouse model, a different virus strain, and reactivation induced by hyperthermia (33), it is apparent that very few neurons (often only one or two per ganglion) become positive for virus antigens after a reactivating stimulus. Nevertheless, we have shown that such an event is sufficient to produce significant virus shedding in the eye and clinical ocular disease (34, 37, 38). The characteristically small numbers of β-Gal-expressing neurons seen after UV irradiation of the cornea suggest that the recombinant virus is capable of reactivation in vivo as well as in vitro (22) and that the incidence of reactivation events in the latently infected TG is similar to that of wild-type viruses.

In conclusion, valuable information on the pathogenesis of HSV infection has been obtained for both primary and reactivated infection by using a combination of a virus carrying a readily detected reporter gene with a tissue mount in which all the major elements involved in the local infection, in the eye and nervous system, can be examined at one time. In particular, it has allowed a greater appreciation of the extent of Schwann cell involvement and the possible role of such involvement in corneal nerves in determining the morphology of the dendritic lesion so characteristic of recurrent epithelial disease of the cornea.

ACKNOWLEDGMENTS

This work was supported by the Medical Research Council, United Kingdom, the National Eye Research Centre, United Kingdom, and the Henry Smith's Charity, United Kingdom.

We are grateful to Jenny Baker, Department of Pathology and Microbiology, University of Bristol, for the electron microscopy and photography.

REFERENCES

1. **Arthur, J. L., C. G. Scarpini, V. Connor, R. H. Lachmann, A. M. Tolkovsky, and S. Efstathiou.** 2001. Herpes simplex virus type 1 promoter activity during latency establishment, maintenance, and reactivation in primary dorsal root neurons in vitro. J. Virol. **75:**3885–3895.
2. **Blyth, W. A., D. A. Harbour, and T. J. Hill.** 1984. Pathogenesis of zosteriform spread of herpes simplex virus in the mouse. J. Gen. Virol. **65:**1477–1486.
3. **Card, J. P., L. Rinaman, R. B. Lynn, B. H. Lee, R. P. Meade, R. R. Miselis, and L. W. Enquist.** 1993. Pseudorabies virus infection of the rat central nervous system: ultrastructural characterization of viral replication, transport, and pathogenesis. J. Neurosci. **13:**2515–2539.
4. **Cook, M. L., and J. G. Stevens.** 1973. Pathogenesis of herpetic neuritis and ganglionitis in mice: evidence of intra-axonal transport of infection. Infect. Immun. **7:**272–288.
5. **Cook, S. D., and J. M. Hill.** 1991. Herpes simplex virus: molecular biology and the possibility of corneal latency. Surv. Ophthalmol. **36:**140–148.
6. **Dillard, S. H., W. J. Cheatham, and H. L. Moses.** 1972. Electron microscopy of zosteriform herpes simplex infection in the mouse. Lab. Investig. **26:**391–402.
7. **Dyson, H., C. Shimeld, T. J. Hill, W. A. Blyth, and D. L. Easty.** 1987. Spread of herpes simplex virus within ocular nerves of the mouse: demonstration of viral antigen in whole mounts of eye tissue. J. Gen. Virol. **68:**2989–2995.
8. **Enquist, L. W., P. J. Husak, B. W. Banfield, and G. A. Smith.** 1998. Infection and spread of alphaherpesviruses in the nervous system. Adv. Virus Res. **51:**237–347.
9. **Field, H. J., and T. J. Hill.** 1974. The pathogenesis of pseudorabies virus in mice following peripheral inoculation. J. Gen. Virol. **23:**145–157.
10. **Field, H. J., and T. J. Hill.** 1975. The pathogenesis of pseudorabies virus in mice: virus replication at the inoculation site and axonal uptake. J. Gen. Virol. **26:**145–147.
11. **Herbort, C. P., S. S. Weissman, and D. G. Payan.** 1989. Role of peptidergic neurons in ocular herpes simplex infection in mice. FASEB J. **3:**2537–2541.
12. **Hill, T. J.** 1985. Herpes simplex virus latency, p. 175–240. *In* B. Roizman (ed.), The herpesviruses. Plenum Press, New York, N.Y.
13. **Hill, T. J.** 1987. Ocular pathogenicity of herpes simplex virus. Curr. Eye Res. **6:**1–7.
14. **Hill, T. J., H. J. Field, and A. P. C. Roome.** 1972. Intra-axonal location of herpes simplex virus particles. J. Gen. Virol. **15:**253–255.
15. **Hill, T. J., and H. J. Field.** 1973. The interaction of herpes simplex virus with cultures of peripheral nervous tissue: an electron microscopic study. J. Gen. Virol. **21:**123–133.
16. **Hill, T. J., H. J. Field, and W. A. Blyth.** 1975. Acute and recurrent infection with herpes simplex virus in the mouse: a model for studying latency and recurrent disease. J. Gen. Virol. **28:**341–353.
17. **Holland, D. J., M. Miranda-Saksena, R. A. Boadle, P. Armati, and A. L. Cunningham.** 1999. Anterograde transport of herpes simplex virus proteins in axons of peripheral human fetal neurons: an immunoelectron microscopy study. J. Virol. **73:**8503–8511.
18. **Jerome, K. R., R. Fox, Z. Cheng, A. Sears, H.-Y. Lee, and L. Corey.** 1999. Herpes simplex virus inhibits apoptosis through the action of two genes, Us5 and Us3. J. Virol. **73:**8950–8957.
19. **Kaye, S. B., C. Shimeld, E. Grinfeld, N. J. Maitland, T. J. Hill, and D. L. Easty.** 1992. Non-traumatic acquisition of herpes simplex virus through the eye. Br. J. Ophthalmol. **76:**412–418.
20. **Kristensson, K., E. Lycke, and J. Sjöstrand.** 1971. Spread of herpes simplex virus in peripheral nerves. Acta Neuropathol. **17:**44–53.
21. **Lachmann, R. H., and S. Efstathiou.** 1997. Utilization of the herpes simplex virus type 1 latency associated regulatory region to drive stable reporter gene expression in the nervous system. J. Virol. **71:**3197–3207.
22. **Lachmann, R. H., M. Sadarangani, H. R. Atkinson, and S. Efstathiou.** 1999. An analysis of herpes simplex virus gene expression during latency establishment and reactivation. J. Gen. Virol. **80:**1271–1282.
23. **LaVail, J. H., K. S. Topp, P. A. Giblin, and J. A. Garner.** 1997. Factors that contribute to the transneuronal spread of herpes simplex virus. J. Neurosci. Res. **49:**485–496.
24. **Ljungdhal, A., K. Kristensson, J. M. Lundberg, E. Lycke, B. Svennerholm, and R. Ziegler.** 1986. Herpes simplex virus infection in capsaicin-treated mice. J. Neurol. Sci. **72:**223–230.
25. **Lohmann, A. M., L. J. Müller, E. Pels, P. G. H. Mulder, and L. Remeijer.** 1999. Corneal epithelial nerves are the anatomic basis for the dendritic figure caused by herpes simplex virus. Investig. Ophthalmol. Vis. Sci. **40:**S549.
26. **Lycke, E., K. Kristensson, B. Svennerholm, A. Vahlne, and R. Zeigler.** 1984. Uptake and transport of herpes simplex virus in neurites of rat dorsal root ganglia cells in culture. J. Gen. Virol. **65:**55–64.
27. **Margolis, T. M., C. R. Dawson, and J. H. LaVail.** 1992. Herpes simplex viral infection of the mouse trigeminal ganglion. Investig. Ophthalmol. Vis. Sci. **33:**259–267.
28. **McCracken, R. M., J. B. McFerran, and C. Dow.** 1973. The neural spread of pseudorabies virus in calves. J. Gen. Virol. **20:**17–28.
29. **Mirsky, R., and K. R. Jessen.** 1986. The biology of non-myelin-forming Schwann cells. Ann. N. Y. Acad. Sci. **486:**132–146.
30. **Müller, L. J., L. Pels, and G. F. J. M. Vrensen.** 1996. Ultrastructure of human corneal nerves. Investig. Ophthalmol. Vis. Sci. **37:**476–488.
31. **Penfold, M. E. T., P. Armati, and A. L. Cunningham.** 1994. Axonal transport of herpes simplex virions to epidermal cells: evidence for a specialized mode of virus transport and assembly. Proc. Natl. Acad. Sci. USA **91:**6529–6533.
32. **Sanna, P. P., T. J. Deerinck, and M. H. Ellisman.** 1999. Localization of a passively transferred human recombinant monoclonal antibody to herpes simplex virus glycoprotein D to infected nerve fibers and sensory neurons in vivo. J. Virol. **73:**8817–8823.
33. **Sawtell, N. M., and R. L. Thompson.** 1992. Rapid in vivo reactivation of herpes simplex virus in latently infected murine ganglionic neurons after transient hypothermia. J. Virol. **66:**2150–2156.
34. **Shimeld, C., T. Hill, B. Blyth, and D. Easty.** 1989. An improved model of recurrent herpetic eye disease in mice. Curr. Eye Res. **8:**1193–1205.
35. **Shimeld, C., T. J. Hill, W. A. Blyth, and D. L. Easty.** 1990. Passive immunization protects the mouse eye from damage after herpes simplex virus infection by limiting spread of virus in the nervous system. J. Gen. Virol. **71:**681–687.
36. **Shimeld, C., J. L. Whiteland, S. M. Nicholls, E. Grinfeld, D. L. Easty, H. Gao, and T. J. Hill.** 1995. Immune cell infiltration and persistence in the mouse trigeminal ganglion after infection of the cornea with herpes simplex virus type 1. J. Neuroimmunol. **61:**7–16.
37. **Shimeld, C., J. L. Whiteland, S. M. Nicholls, D. L. Easty, and T. J. Hill.** 1996. Immune cell infiltration in corneas of mice with recurrent herpes simplex virus disease. J. Gen. Virol. **77:**977–985.
38. **Shimeld, C., D. L. Easty, and T. J. Hill.** 1999. Reactivation of herpes simplex virus type 1 in the mouse trigeminal ganglion: an in vivo study of virus antigen and cytokines. J. Virol. **73:**1767–1773.
39. **Snedecor, G. W., and W. G. Cochran.** 1967. Statistical methods, 6th ed. Iowa State University Press, Ames, Iowa.
40. **Stanberry, L. R.** 1990. Capsaicin interferes with the centrifugal spread of virus in primary and recurrent genital herpes simplex virus infections. J. Infect. Dis. **162:**29–34.
41. **Thackray, A. M., and H. J. Field.** 2000. The effects of antiviral therapy on the distribution of herpes simplex virus type 1 to ganglionic neurons and its consequences during, immediately following and several months after treatment. J. Gen. Virol. **81:**2385–2396.
42. **Tullo, A. B., C. Shimeld, W. A. Blyth, T. J. Hill, and D. L. Easty.** 1982. Spread of virus and distribution of latent infection following ocular herpes simplex

in the non-immune and immune mouse. J. Gen. Virol. **63:**95–101.
43. **Tullo, A. B., D. L. Easty, T. J. Hill, and W. A. Blyth.** 1982. Ocular herpes simplex and the establishment of latent infection. Trans. Ophthalmol. Soc. UK **102:**15–18.
44. **Tullo, A. B., C. Shimeld, W. A. Blyth, T. J. Hill, and D. L. Easty.** 1983. Ocular infection with herpes simplex virus in nonimmune and immune mice. Arch. Ophthalmol. **101:**961–964.
45. **Wilkinson, R., C. Leaver, A. Simmons, and R. A. Pereira.** 1999. Restricted replication of herpes simplex virus in satellite glial cell cultures clonally derived from adult mice. J. Neurovirol. **5:**384–391.
46. **Worrell, J. T., and C. J. Cockerell.** 1997. Histopathology of peripheral nerves in cutaneous herpesvirus infection. Am. J. Dermatol. **19:**133–137.
47. **Zander, E., and G. Weddell.** 1951. Observations on the innervation of the cornea. J. Anat. **85:**68–99.